



UNIVERSITY OF LEEDS

This is a repository copy of *A biocompatible decellularized pulp scaffold for regenerative endodontics*.

White Rose Research Online URL for this paper:
<http://eprints.whiterose.ac.uk/125337/>

Version: Accepted Version

Article:

Matoug-Elwerfelli, M, Duggal, MS, Nazzal, H orcid.org/0000-0002-6220-8873 et al. (2 more authors) (2018) A biocompatible decellularized pulp scaffold for regenerative endodontics. *International Endodontic Journal*, 51 (6). pp. 663-673. ISSN 0143-2885

<https://doi.org/10.1111/iej.12882>

© 2017 International Endodontic Journal. Published by John Wiley & Sons Ltd. This is the peer reviewed version of the following article: Matoug-Elwerfelli M, Duggal MS, Nazzal H, Esteves F, Raif E. A biocompatible decellularized pulp scaffold for regenerative endodontics. *International Endodontic Journal*, 51, 663–673, 2018. , which has been published in final form at <https://doi.org/10.1111/iej.12882>. This article may be used for non-commercial purposes in accordance with Wiley Terms and Conditions for Self-Archiving. Uploaded in accordance with the publisher's self-archiving policy.

Reuse

Items deposited in White Rose Research Online are protected by copyright, with all rights reserved unless indicated otherwise. They may be downloaded and/or printed for private study, or other acts as permitted by national copyright laws. The publisher or other rights holders may allow further reproduction and re-use of the full text version. This is indicated by the licence information on the White Rose Research Online record for the item.

Takedown

If you consider content in White Rose Research Online to be in breach of UK law, please notify us by emailing eprints@whiterose.ac.uk including the URL of the record and the reason for the withdrawal request.



eprints@whiterose.ac.uk
<https://eprints.whiterose.ac.uk/>

A biocompatible decellularized pulp scaffold for regenerative endodontics

M. Matoug-Elwerfelli¹, M. S. Duggal², H. Nazzal³, F. Esteves⁴ & E. Raif¹

¹Division of Oral Biology, School of Dentistry, University of Leeds, Leeds, UK; ²Discipline of Orthodontics and Paediatric Dentistry, National University Health System, Singapore, Singapore; ³Department of Paediatric Dentistry, School of Dentistry, University of Leeds; and ⁴Leeds Institute of Cancer and Pathology, St James University Hospital, Leeds, UK

Correspondence: M. S. Duggal, Discipline of Orthodontics and Paediatric Dentistry, National University Health System, 11 Lower Kent Ridge Road, 119083 Singapore, Singapore (e-mail: denmasd@nus.edu.sg).

Abstract

Aim To investigate the feasibility of decellularizing the entire dental pulp using a mild treatment protocol to develop a decellularized biological extracellular matrix scaffold for use in regenerative endodontic procedures.

Methodology Decellularized human dental pulps were assessed using histological and immunohistochemical methods, scanning electron microscope and DNA quantification assay. Cytotoxicity assays to determine decellularized scaffold biocompatibility were also performed. Decellularized scaffolds were seeded with human dental pulp stem cells and cell viability assessed using Live/Dead[®] stain. Quantitative data were analysed statistically using Student's t-test and one-way analysis of variance to compare mean values between groups depending on group numbers.

Results Assessment of decellularized tissues revealed an acellular matrix with preservation of native tissue histoarchitecture and composition. Decellularized tissues showed no evidence of cytotoxicity, with cell growth in direct contact with the scaffold and no reduction in cellular activity following extract incubation. Furthermore, the scaffold was able to support human dental pulp stem cell viability and attachment following recellularization.

Conclusions Promising results were observed in developing a decellularized biological scaffold derived from the dental pulp with the preservation of extracellular structural components which are required for tissue-specific regeneration.

Keywords: decellularization, dental pulp, extracellular matrix, immature nonvital teeth, regeneration.

Introduction

Dental tissue regeneration has recently emerged as an exciting new concept in managing immature nonvital pulp (European Society of Endodontology 2016) with several published protocols showing variable outcomes (Nicoloso et al. 2017). These protocols share common steps involving chemical disinfection, utilization of stem cells of the apical papilla and scaffold creation through induction of a blood clot (Galler 2016).

Reviews of the regenerative endodontic procedures, also known as revitalization procedures, have concluded that, although they show promise, the outcomes remain unpredictable (Wigler et al. 2013, Moreno-Hidalgo et al. 2014, Nazzal and Duggal 2017). Despite continuation of root development reported in some studies it is unclear whether such development is the result of stem cell repopulation, revascularization, regeneration or merely maturogenesis (Galler et al. 2011).

Regeneration of a pulp structure is unlikely to be successful unless the basic principles of tissue engineering are implemented within any regenerative endodontic procedure. Such protocols should be aimed at promoting and guiding the development of the desired structures using appropriate stem cells, scaffolds and signalling molecules (Langer and Vacanti 1993).

Various scaffolds have been tested in an attempt to regenerate the pulp-dentine complex, with limited success (Galler et al. 2011). Recently, the use of biological scaffolds composed of an acellular extracellular matrix (ECM) derived through tissue decellularization has been advocated (Gilbert et al. 2006, Crapo et al. 2011, Song and Ott 2011). Decellularization is defined as the efficient removal of all cellular and nuclear contents without negatively affecting ECM composition (Gilbert et al. 2006, Badylak et al. 2009).

Preservation of this nanostructured environment and network mesh of fibrous and adhesive proteins provide cell anchorage and regulates future cellular activities (Martinez et al. 2000, Galler et al. 2011). The natural tissue matrix is considered as the ideal scaffold for tissue regeneration (Badylak 2002) and the creation of an acellular scaffold that is able to attract and support local resident cells is a possible direction for pulp-dentine tissue engineering (Galler et al. 2011).

Within the dental field attempts to decellularize porcine tooth buds (Traphagen et al. 2012, Zhang et al. 2017), pulp tissues obtained from miniature swine teeth (Chen et al. 2015) and human pulp tissues within root slices (Song et al. 2017) have been recently reported. Chen et al. (2015) and Song et al. (2017) reported successful decellularization of dental tissues utilising 1% sodium dodecyl sulphate (SDS) and 1% Triton X-100. Despite these results, the use of decellularization protocols with lower concentrations of toxic detergents is advantageous for future tissue regeneration.

Therefore, the aim of this work was to assess the feasibility of decellularizing the whole dental pulp using a single cycle of lower concentrations of SDS (0.03%) to develop a decellularized biological ECM scaffold for use in regenerative endodontic procedures.

Materials and methods

All chemicals, reagents, cell culture medium and supplements were purchased from Sigma-Aldrich (Poole, UK) and cell culture plastics were obtained from Corning® (Amsterdam, the Netherlands) unless stated otherwise.

Tissue procurement

Written informed patient consent and ethical approval were obtained from Skeletal Research Tissue Bank; reference number 101013/MME/113 (School of Dentistry, University of Leeds, Leeds, UK). Clinically sound human premolars (donor's age 11-30 years) were collected within 48 h following extraction, and pulp tissues were aseptically retrieved and stored in 0.1 M phosphate-buffered saline (PBS; Lonza, Slough, UK) at -80 °C.

Decellularization

Pulp tissues were thawed at room temperature and washed thrice in PBS (Lonza) containing aprotinin (10 KIU mL⁻¹). Decellularization protocol used was previously described by Wilshaw et al. (2006). In brief, pulp tissues were incubated in a hypotonic Tris-buffer (10 mM Tris), pH 8.0 containing protease inhibitors [0.1% ethylene-diamine-tetra-acetic acid (EDTA) and aprotinin (10 KIU mL⁻¹)] overnight at 4 °C. Samples were then placed in 0.03% SDS for 24 h at room temperature with

constant shaking. Tissues were washed thrice in Tris-buffered saline and incubated in a reaction buffer [Tris-hydrochloric acid (50 mM), pH 7.5 with magnesium chloride (10 mM) and bovine serum albumin (50 $\mu\text{g mL}^{-1}$)] containing DNase (50 U mL^{-1}) and RNase (1 U mL^{-1}) for 3 h at 37 °C. Finally, tissues were disinfected with 0.1% peracetic acid for 3 h and washed thrice in Tris-buffered saline.

Histology and immunohistochemistry analysis

Control (untreated) and study (decellularized) tissues (n = 4/group) were fixed in 10% neutral-buffered formalin (Cellpath, Wales, UK) for 24 h. The fixed tissues were embedded in 2% agar, dehydrated using an automated tissue processor (ASP200; Leica Biosystems, Newcastle Upon Tyne, UK) and embedded in paraffin wax. Paraffin-embedded blocks were serial sectioned at 4 μm thickness.

Tissue sections were stained with hematoxylin and eosin (H&E; Thermo Fisher Scientific, Loughborough, UK) to evaluate tissue histoarchitecture and 4',6-diamidino-2-phenylindole (DAPI; Vector Labs, Peterborough, UK) to assess nucleic acids. Alcian blue (TCS Biosciences Ltd, Buckingham, UK) and picrosirius red (Polysciences Inc, Warrington, USA) stains were used to visualise acidic polysaccharides and collagen fibres, respectively.

Immunohistochemistry slides were initially subjected to antigen retrieval methods. Antigen retrieval for mouse anticollagen type I and anticollagen type III antibodies were performed by heat retrieval for 2 minutes under full pressure using automated electrical pressure cook (MenaPath, Winnersh-Wokingham, UK) using Tris-EDTA buffer solution (pH 9.0) or citric acid buffer solution (pH 6.0), respectively, whilst antigen retrieval for both rabbit antilaminin and mouse antifibronectin antibodies were performed using bond enzyme pre-treatment kit (Leica Biosystems, Newcastle Upon Tyne, UK) by incubating slides for 15 min at 37 °C.

Slides were then incubated for 1 h at room temperature with the following primary antibodies and isotype controls including monoclonal mouse antibodies anticollagen type I (ab90395, 1 : 100; Abcam, Cambridge, UK), anticollagen type III (ab6310, 1 : 200; Abcam), antifibronectin (ab6328, 1 : 50; Abcam), anti-human leukocyte antigen (M0775, 1 : 250; Dako, Glostrup, Denmark) and

polyclonal rabbit antilaminin (NB300-144, 1 : 400; NovusBio, Oxon, UK). Isotype-specific control antibodies IgG (ab199507, Abcam), IgG1 (ab91353, Abcam) and IgG1 Kappa (M9269, Sigma-Aldrich) were used as negative controls, under the same conditions with omission of primary antibodies. Immunolabelling was performed using ImmPRESS excel peroxidase (Vector Labs) or rabbit polymer horseradish peroxidase (MenaPath) staining kits for all mouse and rabbit antibodies, respectively. Brown chromogen peroxidase substrate 3'diaminobenzidine (DAB) (Vector Labs) was used for antibodies detection and counterstained with hematoxylin.

All sections were examined using a light microscope (AxioVision Rel. 4.8 software; Carl Zeiss) except DAPI-stained sections using a fluorescence microscope (AxioVision Rel. 4.7 software; Carl Zeiss). To further assess collagen structure, picrosirius red-stained sections were also viewed using a polarized microscope (Zen software; Carl Zeiss).

Scanning electron microscope

Control and study tissues (n = 2/group) were fixed in 2.5% glutaraldehyde overnight at 4 °C, and dehydrated in ascending ethanol concentrations. Tissues were then exposed to 50% and 100% hexamethyldisilazane solution and left for evaporation overnight. Samples were then mounted on aluminium stubs, gold sputter coated and viewed under scanning electron microscope (SEM; Hitachi S-3400N, High-Technologies Ltd).

DNA quantification assay

Total DNA was extracted from the control and study tissues (n = 4/group) using the DNeasy Blood and Tissue Kit (Qiagen, Manchester, UK) following manufacture's protocol. DNA was quantified using a NanoDrop™ 1000 spectrophotometer at 260/280 nm (Thermo Fisher Scientific).

Tissue cytotoxicity

Cell culture

Mouse fibroblasts L929 cell line (Oral biology department, University of Leeds, UK) were cultured in Dulbecco's modified Eagle's medium (DMEM) supplemented with 10% foetal bovine serum (Lonza), L-Glutamine (2 mmol L⁻¹) and 1% Penicillin-Streptomycin solution.at 37 °C in 5% CO₂ and air. Medium was changed every three days and cells passaged at 80% confluency.

Human dental pulp stem cells (DPSCs) (Oral biology department, University of Leeds) were obtained with informed patient consent and full ethical approval for human stem cells usage (reference number 101013/MME/113). DPSCs were cultured in Alpha-modified minimum essential medium (α -MEM) (Lonza) supplemented with 10% foetal bovine serum (Lonza), L-Glutamine (2 mmol L⁻¹) and 1% Penicillin-Streptomycin solution.at 37 °C in 5% CO₂ and air. Medium was changed every three days and cells passaged at 80% confluency.

Contact cytotoxicity assay

Decellularized tissues (n = 4) were secured to the centre of six-well culture plates using collagen type I gel (Gibco™, Fisher Scientific). Collagen gel and cyanoacrylate glue and were used as negative and positive controls, respectively. L929 cell lines at a density of 2 x 10⁵ cells mL⁻¹ (4 x 10⁵ cells) were cultured in each well for 48 h. The cells were washed with PBS, fixed with 10% neutral-buffered formalin (Cellpath) and stained with Giemsa solution (VWR International, Leicestershire, UK) for 5 min. The plates were washed with water and left to air dry. Changes in cell growth and morphology were visualised using an Olympus IX 7 inverted light microscope (Cell^B software).

Extract cytotoxicity assay

Decellularized tissues (n = 4) were cut and incubated in DMEM with agitation for 72 h at 37 °C. The extract supernatant was collected and stored at -20 °C until future usage. L929 cell lines at a density of 5 x 10⁴ cells mL⁻¹ (1 x 10⁴ cells) were seeded on 96-well plates and incubated for 24 h. DMEM and 40% dimethyl sulfoxide (DMSO) were used as negative and positive control, respectively. Test extract or controls were added to the appropriate wells and incubated for a further 24 h. Cell viability (relative cellular adenosine triphosphate (ATP) content) was determined using the ATPLite™ assay (PerkinElmer, Inc. Seer Green, UK) following manufacture's protocol.

Cell viability assay

Decellularized human scaffolds ($n = 3$) were recellularized using DPSCs. DPSCs (Passage 5) at a density of 5.5×10^4 cells mL^{-1} (1×10^4 cells) were dynamically seeded using an in-house rotating bioreactor for 24 h. The seeded scaffolds were placed in individual 12-well tissue culture plates containing 2 mL of fresh complete α -MEM and statically cultured for an additional 7 and 14 days. Cell viability was assessed, at both time points, using a commercial Live/Dead[®] stain following manufacture's protocol (Molecular Probes, Paisley, UK). Stained scaffolds were then washed in PBS and viewed under confocal Leica microscope (SP2 PLUS; Leica Microsystems, Milton Keynes, UK).

Statistical analysis

Student's *t*-test and one-way analysis of variance (ANOVA) were used to compare mean values between groups depending on group numbers. All data was analysed using GraphPad Prism (Version 6), and a $p < 0.05$ was considered significant.

Results

Efficiency of tissue decellularization

4',6-diamidino-2-phenylindole staining revealed a high cellular content in the control tissues (Fig. 1a). In contrast, the decellularized tissues showed absence of any visible nuclear material (Fig. 1b). Quantification of residual DNA in decellularized tissues removed an average of 98% (dry weight) of native DNA (Fig. 1c). Furthermore the decellularization protocol resulted in complete removal of human leukocyte antigen (major histocompatibility class II) [Fig. 1(d,e)].

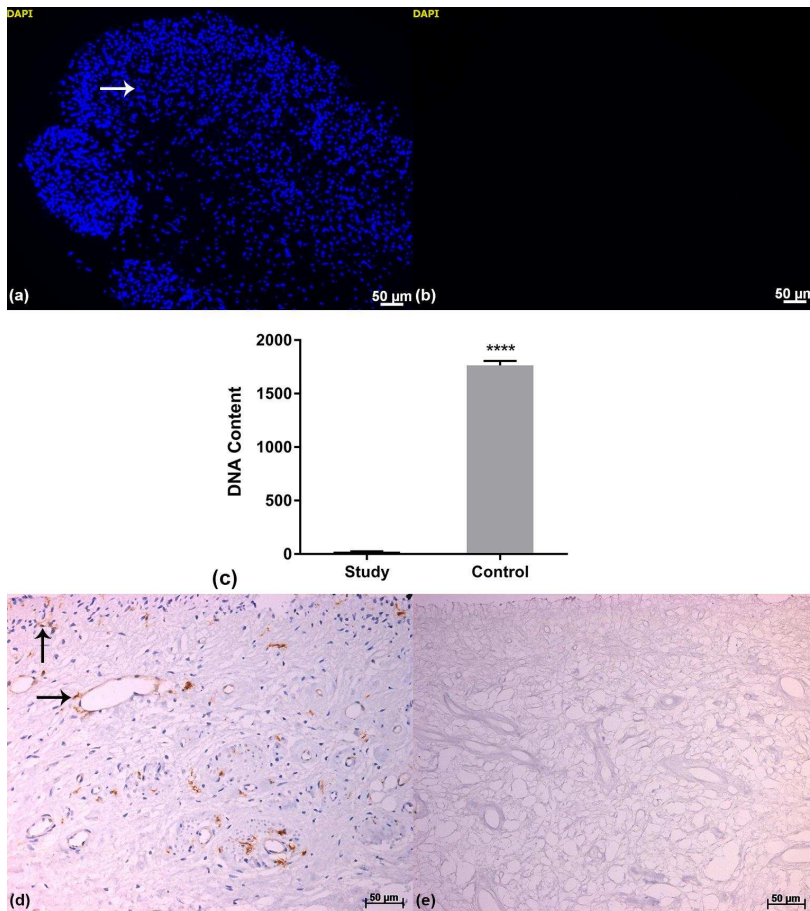


Figure 1: Efficiency of dental pulp decellularization. (a and b) Representative images of DAPI fluorescent stain (a, control and b, decellularized). The images show lack of nuclear material following decellularization. Nuclei stained blue. Scale bar = 50 μm . (c) Bar graph showing results of DNA quantification assay of control and decellularized human pulp tissues. Y-axis DNA content ng mg^{-1} . Data represents mean values ($n = 4$) \pm 95% confidence intervals. The mean DNA measurements in the decellularized tissues contained $19.56 \pm 1.280 \text{ ng.mg}^{-1}$ in comparison to $1182 \pm 56.24 \text{ ng mg}^{-1}$ in the control tissues (t-test, **** $p < 0.0001$). (d and e) Representative images of immunohistochemical stained dental pulp tissues labelled with human leukocyte antigen (major histocompatibility class II) (d, control and e, decellularized). The images revealed complete antigen removal following decellularization. Major histocompatibility class II cells stained brown (black arrow). Scale bar = 50 μm . DAPI, 4',6-diamidino-2-phenylindole.

Tissue structure preservation

H&E staining of the control tissues revealed a highly cellular structure surrounded by loose ECM. Normal pulpal histoarchitecture, with distinct zones (cell free zone, cell rich zone and pulp core), was clearly evident (Fig. 2a). Following decellularization, an acellular loose ECM was evident with preservation of the pulpal histoarchitecture (Fig. 2b).

Picrosirius red staining resulted in a rich porous network of collagen fibres in the control tissues (Fig. 2c). Although the tissue became less dense, decellularization maintained the collagen structure of the dental pulp (Fig. 2d). Under the polarized microscope, abundant collagen bundles, fibres and fibrils

were evident in the control tissues (Fig. 2e). Following decellularization a porous collagen network of various fibre bundles seemed to be preserved (Fig. 2f).

Alcian blue staining revealed an intense staining of acidic polysaccharides in the control tissues (Fig. 2g). The decellularized protocol used resulted in preservation of the acidic polysaccharides contents in the pulp matrix (Fig. 2h).

The decellularized tissues analysed using SEM (Fig. 2J) appeared to be denuded of some components (likely cells) compared to the control (Fig. 2I). Despite the above alteration, no visible change in fibre density or orientation was observed, as the fibre mesh remained dense and irregular.

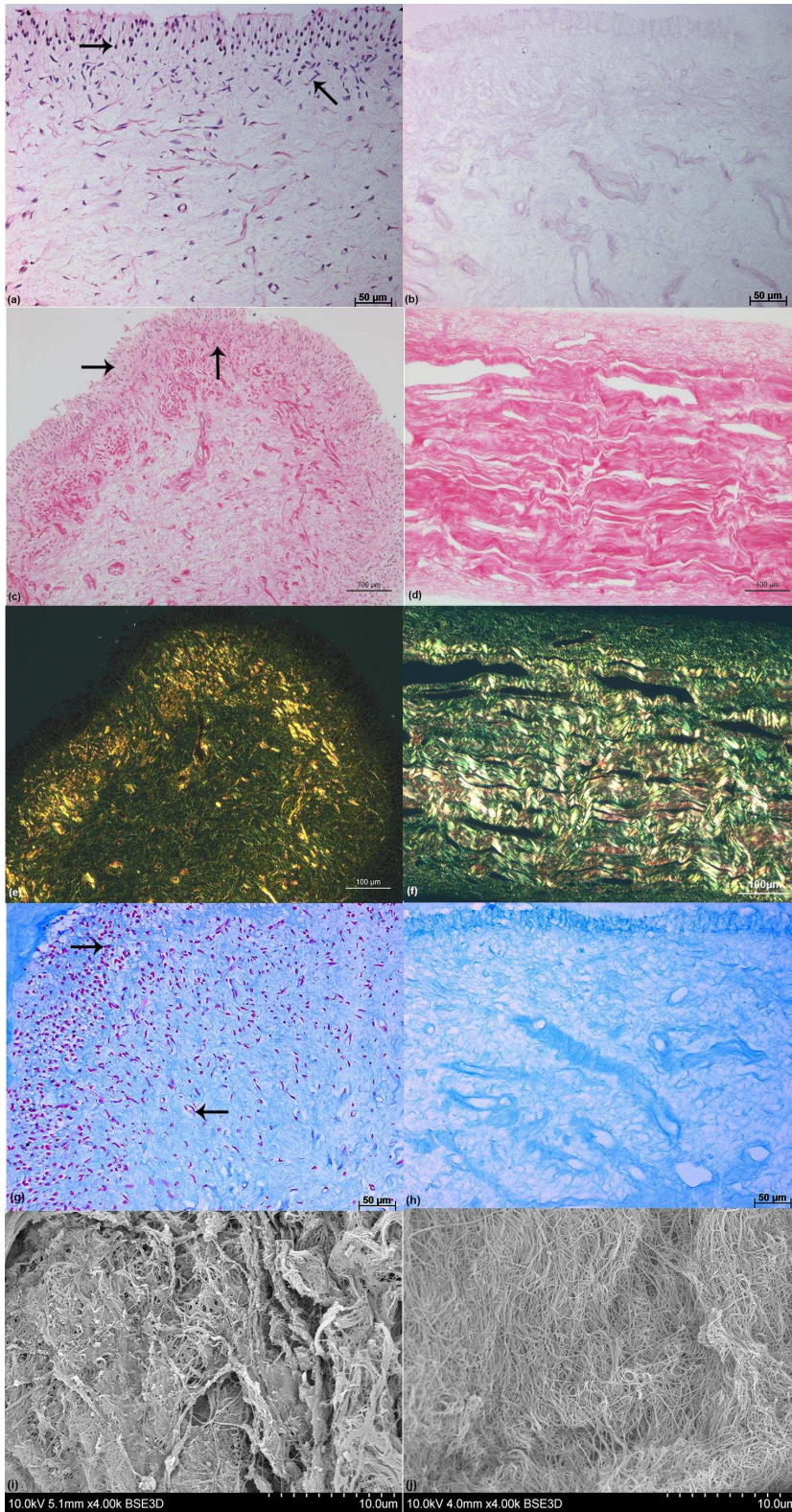


Figure 2: Structure preservation analysis. (a - h) Representative images of histological-stained dental pulp tissues showing H&E (a, control and b, decellularized), picrosirius red (c, control and d, decellularized), picrosirius red under polarized microscope (e, control and f, decellularized) and alcian blue (g, control and h, decellularized) staining. The images revealed preservation of ECM structure following decellularization. Nuclei material (black arrow). Scale bar = 50 μm , except c - f scale bar = 100 μm . (i and j) Scanning electron microscope images of the dental pulp tissues (i, control and j, decellularized). The images revealed preservation of a dense and irregular fibre mesh following decellularization. Scale bar = 10 μm . ECM, extracellular matrix.

Tissue composition

The immunolabelling of collagen type I and III showed a strong intense staining of a rich network of collagen fibres in the control tissues [Fig. 3(a,c)]. Following decellularization the distribution and quality of the collagen structure was largely retained [Fig. 3(b,d)].

In the control tissues, fibronectin labelling appeared as a fibrous plexus throughout the matrix with dense concentration around blood vessels, while laminin labelling was seen mostly around the blood vessels [Fig. 3(e,g)]. Although the immunolabelling of fibronectin and laminin following decellularization was less intense, the pattern of staining and distribution were not altered [Fig. 3(f,h)].

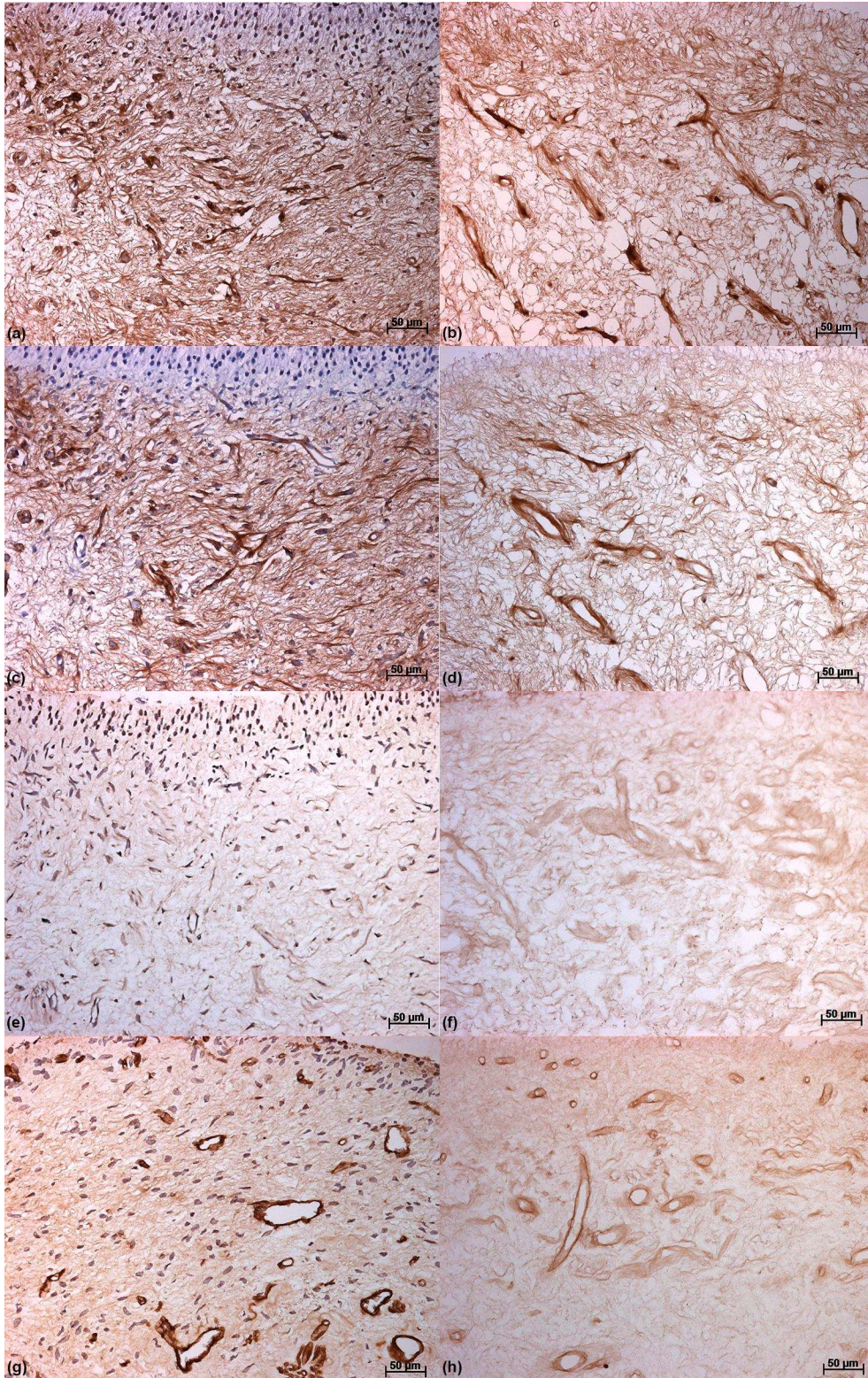


Figure 3: Tissue composition analysis. Representative images of immunohistochemical-stained dental pulp tissues labelled with anticollagen type I (a, control and b, decellularized), anticollagen type III (c, control and d, decellularized), antifibronectin (e, control and f, decellularized), antilaminin (g, control and h, decellularized). The images revealed preservation of structural components following decellularization. Scale bar = 50 µm.

Tissue cytotoxicity

Cytotoxicity assays

Microscope analysis of contact cytotoxicity assay following 48 h culture resulted in no cytotoxicity with no difference in cell growth and morphology between decellularized tissues and negative controls (collagen gel) [Fig. 4 (a,b)]. In contrast, positive controls (cyanoacrylate glue) caused marked cytotoxicity with cell lysis and zones of no cell growth (Fig. 4c). Extracts of decellularized tissues showed no statistical significance difference in cellular ATP content compared with negative controls (DMEM). Statistical significance was seen in the positive controls (DMSO) with an almost complete loss of cellular ATP content ($p < 0.05$, ANOVA) (Fig. 4d).

Cell viability assay

The viability of human DPSCs seeded on the decellularized scaffold was assessed following 7 and 14 days culture. Multiple level constructed (Z-stack) confocal images of Live/Dead[®] stain demonstrated that most areas of the decellularized pulp scaffolds were populated with viable cells exhibiting an elongated morphology and scarcely cells were dead [Fig. 4 (e,f)]. Therefore the recellularized scaffolds were able to support growth and proliferation of DPSCs in culture.

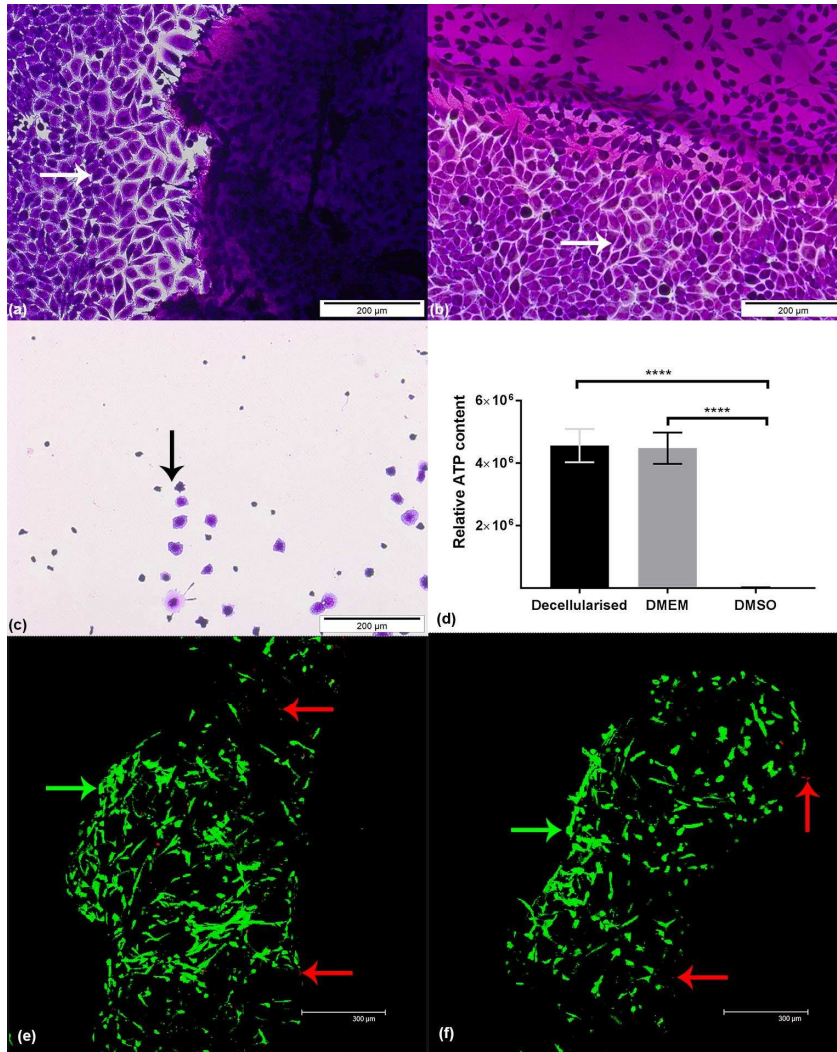


Figure 4: Cytotoxicity analysis. (a - c) Contact cytotoxicity assay cultured with L929 cell line for 48 h and stained with Giemsa stain. (c) Decellularized human pulp tissues resulted in no cytotoxicity with cell growth surrounding and in contact with pulp tissues. (b) Collagen gel (negative control) resulted in no cytotoxicity. (c) Cyanoacrylate glue (positive control) resulted in cell lysis and necrosis. Cell growth and proliferation (white arrow), cell death (black arrow). Scale bar = 200 μ m. (d) Bar graph showing results of extract cytotoxicity assay measuring the relative cellular ATP content of L929 cells incubated in decellularized tissue extracts, DMEM (negative control) and DMSO (positive control) following 24 hour culture. Y-axis relative cellular ATP measurements. Data represents mean values ($n = 4$) \pm 95% confidence intervals. Data analysis revealed no significance difference between decellularized extracts and DMEM (ANOVA, $p > 0.05$) and statistical significance in comparison to DMSO (ANOVA, **** $p < 0.0001$). (e and f) Cell viability assessment of decellularized human scaffolds seeded with human DPSCs and stained using Live/Dead[®] stain. Z-stack images revealed large areas of staining with calcein-AM (green, live cells) and minimal areas of staining with ethidium homodimer (red, dead cells) on the scaffolds following (e) 7 days and (f) 14 days culture. Scaffolds were observed under laser confocal microscope. Live cells (green arrow) and dead cells (red arrow). Scale bar = 300 μ m. DMEM, Dulbecco's modified Eagle's medium; DMSO, dimethyl sulfoxide.

Discussion

The widespread interest in regenerative endodontic procedures, also known as revitalization, has been followed by a period of consideration of the evidence regarding its outcome. Recently published systematic review and meta-analysis have shown that current published evidence is unable to provide definitive conclusions on the predictability of this technique (Tong et al. 2017). Indeed prospective studies have failed to predictably demonstrate any significant hard tissue gain in the root canal system (Nazzal and Duggal 2017). One of the reasons seems to be that the current techniques do not always follow the “gold standard” criteria for the bioengineering of the pulp–dentine complex, with one of the crucial factors being the selection of an appropriate scaffold for successful tissue regeneration (Murray et al. 2007). The development of a decellularized scaffold with complete elimination of donor cells and antigens while preserving ECM structure could provide an excellent platform for tissue regeneration (Badylak 2007). These nonimmunogenic and biocompatible scaffolds conserve native intact structures thereby providing specific microenvironment for cell population and tissue regeneration (Badylak 2007). The decellularized scaffolds could be easily adapted for root canal delivery and used in regenerative endodontics, possibly providing a more controlled regeneration environment for stem cells to differentiate into odontoblasts rather than cementoblasts and/or osteoblasts (Wang et al. 2010, Shimizu et al. 2013, Becerra et al. 2014). It is conceivable that this approach would provide a more suitable environment for regeneration rather than revitalization with better success rates in terms of continuation of root development and thickening of dentinal walls.

Recently, decellularization of the pulp, using human tooth slices, which were essentially pulp–dentine disks 1.5 mm in thickness, has been reported (Song et al. 2017). In contrast the present study reports decellularization of the whole pulp retrieved from extracted teeth. Song et al. (2017) evaluated three different protocols for decellularization, the most effective protocol being the one which incorporated 3 cycles of 1% SDS and 1 cycle of 1% Triton X-100. Similar detergents were also used by Chen et al. (2015). While Triton X-100 (non-ionic detergent) is reported to be more effective in cell removal from thin tissues, some disruption of the ultrastructure and removal of GAGs has been reported (Gilbert et al. 2006, Crapo et al. 2011). SDS (an ionic detergent) is also considered an effective

detergent for cellular and nuclear membrane solubilization; however, concerns regarding the potential toxicity and tissue damage have been reported with the use of 1% SDS on porcine aortic valve (Bodnar et al. 1986). Reducing the concentration of SDS to a 10-fold lower strength (0.1% SDS) was reported to be successful to decellularise human pericardial matrix (Mirsadraee et al. 2006). However, increasing the number of SDS cycles has been shown to cause a reduction in glycosaminoglycans content of the porcine cartilage bone matrix (Kheir et al. 2011).

To overcome the limitations arising when using the above chemicals we deemed it appropriate to evaluate the ability of a previously described decellularization protocol (Wilshaw et al. 2006) that combines a single cycle of freeze-thaw, 0.03% SDS in hypotonic buffer for 24 h, and nuclease enzymatic treatment.

The DNA removal efficiency (approximately 98% of DNA content) in this study was comparable to that reported by Song et al. (2017) in spite of using a single cycle of SDS at 33 times lower concentration and without the use of Triton X-100. The sufficient removal of cellular materials is an important step for future clinical usage as remaining materials could act as foreign body triggering a host immune reaction (Wilshaw et al. 2012). The approximate 20 ng mg^{-1} residual DNA in this study is less than the benchmark criteria for the maximum amount (50 ng mg^{-1}) of DNA content in sufficiently decellularised tissues (Crapo et al. 2011).

Dental pulp ECM is described as a loose connective tissue matrix, composed of collagen fibres and adhesive proteins which contribute towards various cellular interactions and tissue survival (Linde 1985, Goldberg and Smith 2004). In this respect, the decellularization protocol used in this study resulted in preservation of acidic polysaccharides, fibronectin and laminin distribution with minimal alterations in tissue structure and morphology.

Despite the reduction in irregular network fibre density, the collagen pattern distribution was preserved. Gilbert et al. (2006) reported that collagen is resistant to ionic detergents. Therefore the collagen structure alteration observed is likely due to the use of vehiculating aqueous solutions during Decellularization that could induce swelling and histoarchitectural changes (Oliveira et al. 2013).

Initial cytotoxicity assessment was evaluated using L929 mouse fibroblast cell line for reproducibility and accuracy as mentioned by British standard (British Standard Institute 2009). In vitro cytotoxicity assays were performed to determine the effect of chemical residuals in the decellularized tissue on future cell growth and proliferation. The results indicated a non-toxic tissue, which is linked to the low concentration of SDS and extensive vigorous washing cycles used in this protocol (Wilshaw et al. 2006). Furthermore, the ability of the scaffold to support DPSCs growth and attachment was assessed for future clinical translation. DPSCs were widely dispersed throughout the recellularized scaffold and maintained their viability during the course of the experiment (2 weeks).

Conclusion

It is possible to develop a decellularized biocompatible biological scaffold containing the native ECM structural components required for tissue-specific regeneration. This is the first study to have successfully decellularized the entire human dental pulp, and not merely tooth slices with small amounts of pulp tissue. This is a promising step forward in providing the cells with the correct environment to support pulp-dentine complex regeneration. Further assessment of scaffold cell survival and differentiation is needed before clinical translation.

Acknowledgements

The authors thank Dr Stacy-Paul Wilshaw for his expertise with tissue decellularization and laboratory support. The authors acknowledge extended thanks to Jennifer Graham, Ali Marie, Jaqueline Hudson and Timothy Zoltie for their technical assistance and the Academy of Medical Science for their support.

References

- Badylak, SF (2002). The extracellular matrix as a scaffold for tissue reconstruction. *Seminars in Cell and Developmental Biology*, **13**, 377-83.
- Badylak, SF (2007). The extracellular matrix as a biologic scaffold material. *Biomaterials*, **28**, 3587-93.

Badylak, SF, Freytes, DO ,Gilbert, TW (2009). Extracellular matrix as a biological scaffold material: Structure and function. *Acta Biomaterialia*, **5**, 1-13.

Becerra, P, Ricucci, D, Loghin, S, Gibbs, JL ,Lin, LM (2014). Histologic Study of a Human Immature Permanent Premolar with Chronic Apical Abscess after Revascularization/Revitalization. *Journal of Endodontics*, **40**, 133-9.

Bodnar, E, Olsen, EGJ, Florio, R ,Dobrin, J (1986). Damage of porcine aortic valve tissue caused by the surfactant sodiumdodecylsulphate. *Thoracic and Cardiovascular Surgeon*, **34**, 82-5.

British Standard Institute 2009. Biological evaluation of medical devices. Tests for in vitro cytotoxicity (ISO 10993-5:2009).

Chen, G, Chen, J, Yang, B, Li, L, Luo, X, Zhang, X, et al. (2015). Combination of aligned PLGA/Gelatin electrospun sheets, native dental pulp extracellular matrix and treated dentin matrix as substrates for tooth root regeneration. *Biomaterials*, **52**, 56-70.

Crapo, PM, Gilbert, TW ,Badylak, SF (2011). An overview of tissue and whole organ decellularization processes. *Biomaterials*, **32**, 3233-43.

European Society of Endodontology 2016. European Society of Endodontology position statement: Revitalization procedures. *International Endodontic Journal*.

Galler, KM (2016). Clinical procedures for revitalization: current knowledge and considerations. *International Endodontic Journal*, **49**, 926-36.

Galler, KM, D'souza, RN, Hartgerink, JD ,Schmalz, G (2011). Scaffolds for dental pulp tissue engineering. *Advances in Dental Research*, **23**, 333-9.

Gilbert, TW, Sellaro, TL ,Badylak, SF (2006). Decellularization of tissues and organs. *Biomaterials*, **27**, 3675-83.

Goldberg, M ,Smith, AJ (2004). Cells and extracellular matrices of dentin and pulp: a biological basis for repair and tissue engineering. *Critical Reviews in Oral Biology and Medicine*, **15**, 13-27.

Kheir, E, Stapleton, T, Shaw, D, Jin, Z, Fisher, J ,Ingham, E (2011). Development and characterization of an acellular porcine cartilage bone matrix for use in tissue engineering. *Journal of Biomedical Materials Research Part A*, **99**, 283-94.

Langer, R ,Vacanti, J (1993). Tissue engineering. *Science*, **260**, 920-6.

Linde, A (1985). Cells and extracellular matrices of the dental pulp. *Journal of Dental Research*, **64**, 523-9.

Martinez, EF, De Souza, SOM, Corrêa, L ,De Araújo, VC (2000). Immunohistochemical localization of tenascin, fibronectin, and type III collagen in human dental pulp. *Journal of Endodontics*, **26**, 708-11.

Mirsadraee, S, Wilcox, HE, Korossis, SA, Kearney, JN, Watterson, KG, Fisher, J, et al. (2006). Development and characterization of an acellular human pericardial matrix for tissue engineering. *Tissue Engineering*, **12**, 763-73.

Moreno-Hidalgo, MC, Caleza-Jimenez, C, Mendoza-Mendoza, A, Iglesias-Linares, A (2014). Revascularization of immature permanent teeth with apical periodontitis. *International Endodontic Journal*, **47**, 321-31.

Murray, PE, Garcia-Godoy, F, Hargreaves, KM (2007). Regenerative endodontics: a review of current status and a call for action. *Journal of Endodontics*, **33**, 377-90.

Nazzal, H, Duggal, MS (2017). Regenerative endodontics: a true paradigm shift or a bandwagon about to be derailed? *European Archives of Paediatric Dentistry*, **18**, 3-15.

Nicoloso, GF, Pötter, IG, Rocha, RDO, Montagner, F, Casagrande, L (2017). A comparative evaluation of endodontic treatments for immature necrotic permanent teeth based on clinical and radiographic outcomes: a systematic review and meta-analysis. *International Journal of Paediatric Dentistry*, **27**, 217-27.

Oliveira, AC, Garzón, I, Ionescu, AM, Carriel, V, De La Cruz Cardona, J, González-Andrades, M, et al. (2013). Evaluation of small intestine grafts decellularization methods for corneal tissue engineering. *PloS One*, **8**, e66538.

Shimizu, E, Ricucci, D, Albert, J, Alobaid, AS, Gibbs, JL, Huang, GTJ, et al. (2013). Clinical, Radiographic, and Histological Observation of a Human Immature Permanent Tooth with Chronic Apical Abscess after Revitalization Treatment. *Journal of Endodontics*, **39**, 1078-83.

Song, JJ, Ott, HC (2011). Organ engineering based on decellularized matrix scaffolds. *Trends in Molecular Medicine*, **17**, 424-32.

Song, JS, Takimoto, K, Jeon, M, Vadakekalam, J, Ruparel, NB, Diogenes, A (2017). Decellularized human dental pulp as a scaffold for regenerative endodontics. *Journal of Dental Research*, **96**, 640-6.

Tong, HJ, Rajan, S, Bhujel, N, Kang, J, Duggal, M, Nazzal, H (2017). Regenerative Endodontic Therapy in the Management of Nonvital Immature Permanent Teeth: A Systematic Review-Outcome Evaluation and Meta-analysis. *Journal of Endodontics*, **43**, 1453- 64.

Traphagen, SB, Fourligas, N, Xylas, JF, Sengupta, S, Kaplan, DL, Georgakoudi, I, et al. (2012). Characterization of natural, decellularized and reseeded porcine tooth bud matrices. *Biomaterials*, **33**, 5287-96.

Wang, X, Thibodeau, B, Trope, M, Lin, LM, Huang, GTJ (2010). Histologic Characterization of Regenerated Tissues in Canal Space after the Revitalization/Revascularization Procedure of Immature Dog Teeth with Apical Periodontitis. *Journal of Endodontics*, **36**, 56-63.

Wigler, R, Kaufman, AY, Lin, S, Steinbock, N, Hazan-Molina, H, Torneck, CD (2013). Revascularization: a treatment for permanent teeth with necrotic pulp and incomplete root development. *Journal of Endodontics*, **39**, 319-26.

Wilshaw, SP, Kearney, JN, Fisher, J, Ingham, E (2006). Production of an acellular amniotic membrane matrix for use in tissue engineering. *Tissue Engineering*, **12**, 2117-29.

Wilshaw, SP, Rooney, P, Berry, H, Kearney, JN, Homer-Vanniasinkam, S, Fisher, J, et al. (2012). Development and characterization of acellular allogeneic arterial matrices. *Tissue Engineering Part A*, **18**, 471-83.

Zhang, W, Vazquez, B, Oreadi, D, Yelick, PC (2017). Decellularized tooth bud scaffolds for tooth regeneration. *Journal of Dental Research*, **96**, 516-23.